FIBER-TYPE DEPENDENCE OF STRETCH-INDUCED FORCE ENHANCEMENT IN RAT SKELETAL MUSCLE

KATHRYN A. RAMSEY, BSc, ANTHONY J. BAKKER, PhD, and GAVIN J. PINNIGER, PhD

School of Biomedical, Biomolecular and Chemical Sciences, University of Western Australia, Crawley, Western Australia, 6009, Australia

Accepted 29 March 2010

ABSTRACT: When an active muscle is stretched, the force increases due to strain of contractile and noncontractile proteins. We examined this force enhancement in rat extensor digitorum longus (EDL) and soleus muscles, which differ in their composition of these proteins, and their susceptibility to damage. Small stretches were applied at different velocities during isometric contractions from which we quantified the velocity-dependent contractile and velocity-independent noncontractile contributions to force enhancement. Whereas the contractile contribution was significantly greater in soleus than EDL, the noncontractile force enhancement was significantly greater in EDL than soleus, and increased ≈6-fold after damaging eccentric contractions. The increased contractile stiffness may be functionally beneficial in slow muscle, as resistance to lengthening is fundamental to maintaining posture. Following stretch-induced muscle damage this capacity is compromised, leading to increased strain of noncontractile proteins that may facilitate the activation of signaling pathways involved in muscle adaptation to injury.

Muscle Nerve **42:** 769–777, 2010

The capacity of skeletal muscle to resist being stretched is essential for normal locomotion. The resistance to muscle lengthening, as occurs during eccentric contractions, enables muscle to absorb energy to decelerate body movements, stabilize the body to protect from joint or ligament damage, and store energy that can be utilized during a subsequent shortening (concentric) contraction. The requirement of a muscle to act in this manner may be determined by its type and location in the body. For example, postural muscles such as the soleus are frequently required to resist lengthening in order to maintain balance during standing, whereas the hamstring muscles often act to decelerate the lower limb during the terminal swing phase of running. The failure of these muscles to adequately resist lengthening may compromise normal locomotion and/or predispose a muscle to stretch-induced damage. Therefore, it is relevant to investigate the ability of different muscle types to resist lengthening.

When actively contracting muscle is lengthened, the force it exerts is enhanced above the isometric force at the corresponding length. The force enhancement during stretch is complex in that it has at least two components: a velocity-dependent increase in force that has been attributed to the strain of attached crossbridges, and a velocity-independent increase in force that has been suggested to arise from the strain of noncontractile proteins that reside in the sarcomere.[1–3] After the ramp phase of the stretch, the force decays, but only partially, to reach a new steady-state force that is higher than the isometric force at the corresponding muscle length. This sustained increase in force after stretch is often termed residual force enhancement (RFE) or permanent extra tension.[1,4,5] Although numerous studies have characterized the different components of stretch-induced force enhancement, the underlying mechanisms, in particular those that give rise to the velocity-independent component, remain controversial.[2,6–8]

Examination of the velocity-dependent increase in force at the onset of stretch has provided valuable insight into the mechanisms of muscle contraction.[4,9–15] This force transient is dominated by a steep initial increase in force followed (usually) by a slower force rise. It has been investigated in a range of muscle preparations from cat whole muscle[16] to single skinned rabbit fibers.[17] The transition between these two phases occurs at a constant amplitude (i.e., after ≈8–20 nm per half-sarcomere), and the force at this transition displays a velocity-dependence up to a critical velocity that is influenced by crossbridge cycling kinetics. Flitney and Hirst[10] demonstrated that the change in sarcomere length during the initial, steep tension rise was less than expected based on the ramp characteristics, implying that some of the strain is taken up by noncontractile elastic elements. This is consistent with the observations of Edman and Tsuchiya[6] that the strain of an elastic element contributes to force enhancement during stretch and dominates the slower tension rise after the transition. It has been argued that the noncrossbridge force that develops during the stretch gives rise to the permanent extra tension, or RFE, observed after the stretch.[2,6]

RFE has been demonstrated in a range of preparations from isolated myofibrils[18] to whole human muscles under voluntary activation[19] and, therefore, it must be considered a physiological characteristic of all skeletal muscle. However, the

Abbreviations: BTS, *N*-benzyl-*p*-toluene sulfonamide; CSA, cross-sectional area; DMC, dynamic muscle control software; EDL, extensor digitorum longus; FE, force enhancement; L_m, optimal muscle length; L_o, optimal fiber length; P_o, maximum isometric force; P_L, plateau force from Eq. 1; RFE, residual force enhancement; TnC, troponin C; V_C, critical velocity from Eq. 1

Key words: cross-bridge, force-velocity, muscle damage, cytoskeleton, residual force enhancement

Correspondence to: G.J. Pinniger; e-mail: gavin.pinniger@uwa.edu.au

Published online 15 October 2010 in Wiley Online Library (wileyonlinelibrary.com). DOI 10.1002/mus.21744

crossbridge theory of muscle contraction does not account for RFE, as it states that the steady-state force after a stretch should be independent of its contractile history.[20] It has been suggested that stretching an active muscle could alter the crossbridge interactions that cause the second myosin head to attach to the thin filament,[21] resulting in an increased number of attached myosin heads. An alternative proposal is the transition from weakly bound to strongly bound crossbridges during the stretch resulting in an increased average force per attached crossbridge.[22,23] Either mechanism could account for the increase in steady-state force after a stretch. However, several lines of evidence argue against a crossbridge contribution to RFE. For example, RFE is unaffected by the myosin-II inhibitor *N*-benzyl-*p*-toluene sulfonamide (BTS), which reduces active force production while not affecting the $[Ca^{2+}]_i$ transient.[2,24] Furthermore, the amplitude of RFE is independent of stretch velocity,[2] but increases with the amplitude of the stretch. It has also been demonstrated that RFE is greatest when stretches are applied on the descending limb of the length tension relationship when active force production is decreasing due to reduced filament overlap.[1,5,25]

If RFE cannot be attributed to the contractile proteins, then it must be assumed to originate from the noncontractile proteins within the sarcomere. Noncontractile proteins, such as titin, nebulin, desmin, and dystrophin, are essential for maintaining the myofibrillar arrangement within the muscle and stabilizing the contractile filaments during active contraction.[26] These proteins also generate passive force at long muscle lengths, and the strain of structural proteins, such as titin, has been implicated as the noncontractile origin of RFE.[1,2,5,27–29] Given the fiber-type differences in the composition of noncontractile proteins, including the expression of a shorter, stiffer titin isoform in fast skeletal muscle,[30–34] we hypothesized that the contribution of noncontractile proteins to stretch-induced force enhancement would be greater in fast compared to slow skeletal muscle and that this would contribute to the increased susceptibility of fast muscle to stretch-induced muscle damage.[35]

It is clear that force enhancement during and after stretch is a complex response involving the strain of both contractile and noncontractile components. To further investigate the relative contribution of these components to stretch-induced force enhancement we performed stretches on small longitudinal strips of intact muscle fibers isolated from rat extensor digitorum longus (EDL) and soleus (SOL) muscles. These muscles were chosen because of their composition of fast and slow twitch fibers (EDL 95%–100% fast-twitch[36–38]; SOL 75%–80% slow-twitch fibers[36,38,39]) and the well-defined differences in contractile[40] and noncontractile properties[41] and susceptibility to stretch-induced muscle damage.[35]

MATERIALS AND METHODS

Experiments were performed using EDL and SOL muscles from a total of 37 adult Wistar rats (mean ± SE body weight = 103 ± 24 g). All experiments were conducted with the approval of the University of Western Australia Animal Ethics Committee and conformed to the guidelines of the National Health and Medical Research Council of Australia. Animals were anesthetized with an intraperitoneal injection of sodium pentobarbitone (Lethabarb, 40 mg/kg body weight) such that they were unresponsive to tactile stimuli. The muscles were surgically excised from the animal and dissected into longitudinal strips of whole muscle. For EDL muscles the distal tendon was separated into four distinct branches, and the muscle fibers attached to one of these branches were isolated from the remainder of the whole muscle. For SOL the whole muscle was carefully dissected into longitudinal strips of approximately one-third of the whole muscle width. The tendons of each preparation were tied with braided surgical silk to a fixed hook at one end and to a dual-mode force transducer-servomotor at the other (1200A Intact Muscle Test System, Aurora Scientific, Canada). The muscles were housed in a vertical organ bath containing mammalian Ringer's solution (in mM; NaCl 137, $NaHCO_3$ 24, glucose 11, KCl 5, $CaCl_2$ 2, NaH_2PO_4 1, $MgSO_4$ 1 and d-tubocurarine chloride 0.025, maintained at pH 7.3) and bubbled with carbogen (5% CO_2 in O_2, Air Liquide, Western Australia) at 25°C. The muscle was stimulated (100 Hz) by a 701B stimulator (Aurora Scientific) delivering supramaximal square-wave pulses (0.3 ms) via two platinum electrodes running parallel on either side of the suspended muscle. The force and length output were recorded on a PC using Dynamic Muscle Control (DMC) software (Aurora Scientific). The DMC software also enabled control of position of the lever arm to set the initial muscle length and apply ramp stretches to the muscle at a specific amplitude and velocity. Optimum muscle length (L_m) was determined from micromanipulation of muscle length. The length of the muscle at which the maximum isometric twitch force was recorded was measured using digital calipers and was taken as the L_m. Optimum fiber length (L_o) was estimated based on the ratio of L_m to L_o. Published L_m to L_o ratios for rat skeletal muscle vary widely for both EDL (0.40–0.48[36,38,42])

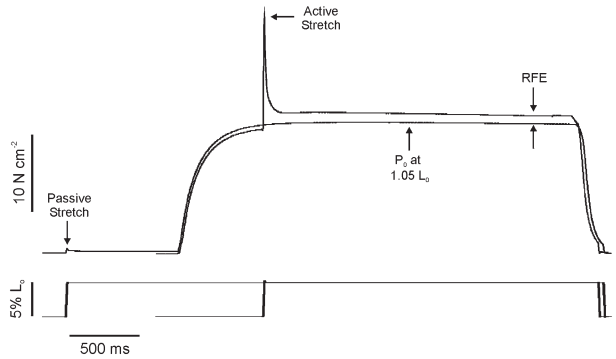

FIGURE 1. Sample recordings of the tension response (upper trace) to a ramp stretch at 5 $L_o s^{-1}$ (lower trace) applied on the plateau of a tetanic contraction in the EDL muscle (Active Stretch). Also shown are the tension recordings when the resting muscle was first stretched to 1.05 L_o (labeled Passive Stretch) and then stimulated to produce an isometric contraction at the longer muscle length (P_o at 1.05 L_o). After the ramp stretch, tension decayed rapidly to reach a new steady-state tension that remained for the duration of stimulation. RFE was measured as the difference between the steady-state tension after the stretch and the isometric tension at 1.05 L_o. RFE from this recording (0.07 P_o) was similar to the mean RFE for all EDL recordings (0.05 P_o).

and SOL (0.52–0.69[36,38,43]) muscles. Therefore, we performed our own estimation of L_m to L_o ratios from longitudinal sections of EDL and SOL muscles under a dissecting microscope. Based on multiple measurements of four EDL and four SOL muscles, the mean (±SE) ratios were 0.46 (±0.01) for EDL and 0.69 (±0.01) for SOL.

At the end of the experiment, muscles were removed from the organ bath, trimmed of their tendons, blotted on filter paper, and weighed on an analytical balance. The recorded muscle weights and L_o were used for the calculation of cross-sectional area (CSA) to enable the calculation of specific force (N/cm^2).

Experimental Protocol. The force-velocity profiles of EDL (n = 10) and SOL (n = 9) muscles were determined by applying small (5% L_o) nondamaging stretches of constant velocity (0.075, 0.1, 0.25, 0.5, 1.0, 2.0, 4.0, 5.0, 7.5, and 10 $L_o s^{-1}$) in a random order on the plateau of an isometric tetanic contraction (P_o) at optimal length (L_o) (Fig. 1). After the stretch the muscle was held at the new longer length, and stimulation was maintained until the force enhancement that developed during the stretch had decayed to a steady-state (1 s for EDL and 2 s for SOL, determined based on analysis of the rate of tension decay after stretch from preliminary experiments; data not shown). An isometric contraction at the longer muscle length (1.05 L_o) was performed after each stretch by first passively stretching the muscle by 5% L_o (at the same constant velocity as for the active stretch) and then stimulating the muscle to record the maximal isometric tetanus. Residual force enhancement was measured as the steady-state force after stretch minus the isometric force (at 1.05 L_o). There was a 3-min interval between each active stretch and isometric contraction to prevent muscle fatigue. The tension response to stretch in the relaxed (passive) muscle was recorded at each velocity and subtracted from the tension record from the stretches of the activated muscle.

The force enhancement during stretch (FE), measured as the peak force during the stretch in excess of the isometric force, was plotted against stretch velocity (Fig. 2). For each individual muscle the crossbridge and noncrossbridge components of FE were determined using the equation below, which is based on an equation by Schoenberg[44] that describes the kinetics of weakly binding crossbridges[2]:

$$FE = P_L (V/V_C) (1 - \exp(-V_C/V)) + C \quad (1)$$

From this equation the crossbridge tension is viscoelastic and reaches a plateau (P_L) at high velocity (V). V_C is a measure of velocity sensitivity, characterizing the velocity beyond which FE becomes insensitive to the rate of stretch[10] and is governed by crossbridge attachment and detachment, and C represents the velocity-independent (noncrossbridge) force, which develops in proportion to the stretch reaching a maximum at the end of the ramp. Curve-fit analysis was performed using Fig. P software (Biosoft, Great Shelford, Cambridgeshire, UK).

The effects of eccentric muscle damage on the contractile and noncontractile contributions to stretch-induced force enhancement were examined in EDL (n = 9) and SOL (n = 9) muscles. In these

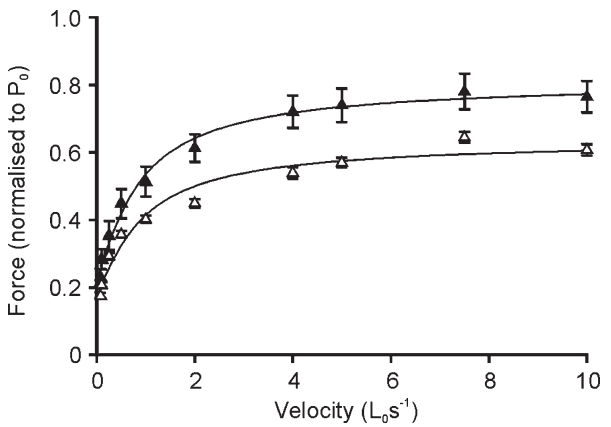

FIGURE 2. Velocity dependence of stretch-induced force enhancement (FE). Mean (±SE) FE for EDL (open symbols; n = 10) and SOL (filled symbols; n = 9) increased steeply at low stretch velocities (<2 $L_o s^{-1}$) and approached a plateau at higher velocities. The continuous line represents the curve-fit from the equation $FE = P_L (V/V_C) (1-\exp(-V_C/V)) + C$.

experiments a single nondamaging stretch (5% L_o at 5 $L_o s^{-1}$) was applied to the plateau of an isometric contraction, and the force record was analyzed to establish predamage values for the slope of the initial tension rise (P_o/L_o) and for RFE. The muscle was then exposed to 10 damaging eccentric contractions (20% L_o at 5 $L_o s^{-1}$, at 3-min intervals) after which changes in slope of the initial tension rise and RFE were examined in the damaged muscle.

Data Analysis. Data were collected using DMC software and imported into Signal 2 (Cambridge Electronic Design, Cambridge, UK) for further analysis. All force measurements were normalized to muscle CSA (N/cm^2) and were also expressed relative to the maximum P_o. Statistical analysis was performed using GraphPad Prism (v. 4.02, GraphPad Software, San Diego, California). Two-way analyses of variance (ANOVAs) with Bonferroni post-hoc analysis were performed to determine the differences in FE, RFE, and passive force between EDL and SOL over the 10 velocities of stretch. Student's one-tailed unpaired *t*-tests were used elsewhere to determine if there were significant differences between group means. In all analyses $P < 0.05$ was regarded as a significant difference.

RESULTS

The maximum specific force (P_o) for EDL (20.1 ± 0.38 N/cm^2) was not significantly different from that of SOL (19.8 ± 0.48 N/cm^2). The increase in passive force after stretch was independent of stretch velocity, therefore, data acquired at all stretch velocities were pooled for comparisons between EDL and SOL. The mean force increase produced by a passive stretch was significantly higher in EDL (0.03 ± 0.002 P_o) than SOL (0.01 ± 0.001 P_o; $P < 0.01$).

The force enhancement during stretch of an active muscle (FE) increased with stretch velocity in both the EDL and SOL ($F_{(1,9)} = 2.54$, $P < 0.01$). The force–velocity curve in Figure 2 displays the mean (±SE) amplitudes of the FE from EDL and SOL plotted over the 10 stretch velocities. The curves fitted to the FE data in Figure 2 were derived from the equation given previously (Materials and Methods), and the parameters determined for the EDL and SOL curves are shown in Figure 3. The mean P_L for SOL was significantly greater than that for EDL ($P < 0.05$), indicating that the contribution of the contractile component to FE was larger in the slow SOL muscle. However, there was no significant difference between EDL and SOL for either the noncontractile contribution to FE (C; $P = 0.08$) or the velocity sensitivity (V_C; $P = 0.06$).

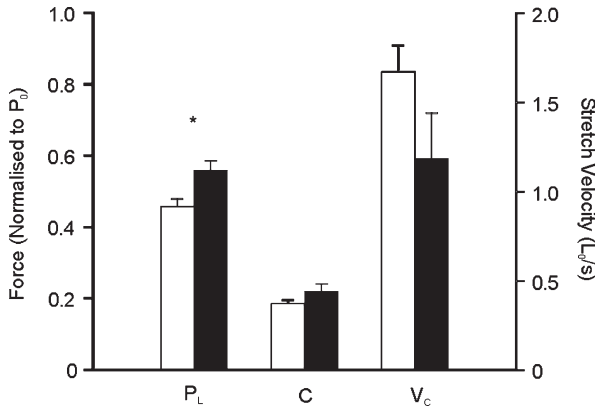

FIGURE 3. Parameters of the curve-fit analysis of contractile and noncontractile contributions to FE. Data are presented as mean ±SE for EDL (open bars) and SOL (filled bars). P_L and C values are as plotted normalized force on the left axis. V_C is plotted as stretch velocity on the right axis. *Significantly different ($P < 0.05$).

At the end of the ramp stretch the force decayed in a complex manner to reach a new steady-state force and remained at this level for the duration of stimulation. The force decay was fit with a biexponential function to characterize a fast component and a slow component of tension decay. The rate of decay of the fast component was sensitive to stretch velocity, but it approached a plateau at velocities greater than 4 $L_o s^{-1}$. At this plateau the rate of force decay for EDL was ≈4-fold higher than for SOL (200/s vs. 50/s, respectively). The rate of decay of the slow component was <10/s for both EDL and SOL and was independent of stretch velocity. Despite differences in the rate of force decay after the stretch, RFE was always measured once a new steady-state force was reached in both EDL and SOL preparations.

RFE, unlike the force enhancement during stretch, was insensitive to stretch velocity ($F_{(1,9)} = 1.64$; $P > 0.05$). As RFE was independent of velocity, the data were pooled across the 10 stretch velocities for each muscle group and are presented in Figure 4. The mean RFE value for EDL was significantly higher than that of SOL ($P < 0.01$). Furthermore, RFE was significantly greater than the stretch-induced passive force in both EDL and SOL ($P < 0.05$).

The force enhancement at the onset of stretch is characterized by a steep linear increase in force until a transition is reached, after which there is a marked reduction in slope (Fig. 5). This biphasic force enhancement has been characterized in previous studies.[1,10,12,13,17,45–47] It is argued that the initial steep tension rise is dominated by the increased strain of attached crossbridges, whereas the latter, shallower rise reflects the strain of noncrossbridge parallel elastic elements. Our analysis of this tension rise revealed a significant difference

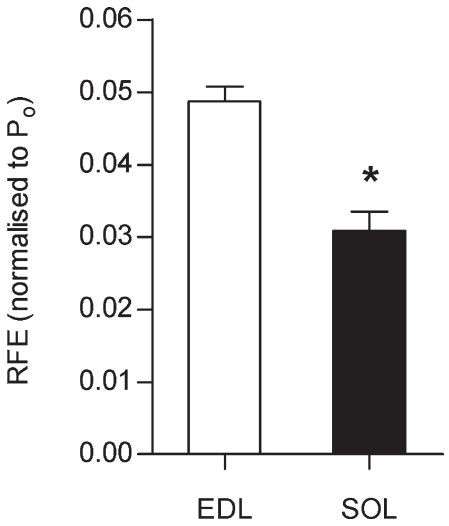

FIGURE 4. Pooled residual force enhancement data for EDL and SOL. Mean ±SE values for RFE pooled across all stretch velocities for EDL (open bars) and SOL (solid bars). *Significantly different from EDL ($P < 0.05$).

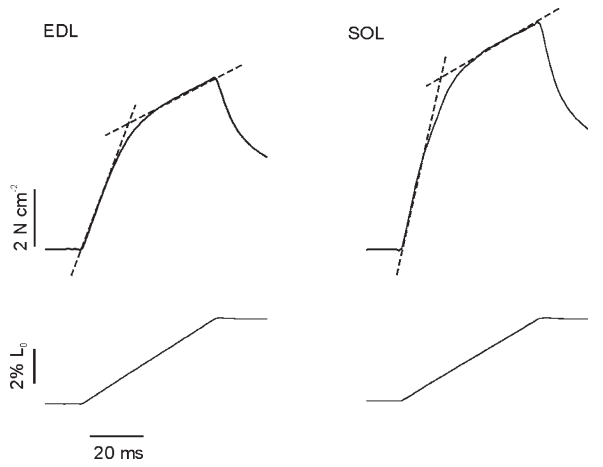

FIGURE 5. Representative traces of the force-enhancement during a stretch at 1 $L_o s^{-1}$ in longitudinal strips of fast (EDL) and slow (SOL) fibers. Two distinct phases were identified on the force record during the stretch. The slope of the initial force increase was greater in SOL than EDL, whereas the slopes of the slower force rise were not significantly different. (The slopes for the initial and later phases in these preparations were 19 and 2.8 P_o/L_o for EDL and 25 and 3.3 P_o/L_o for SOL, which are comparable to the mean data.) The transition of the two phases is characterized by identifying the intersection of two linear regression lines fit to the initial and latter slopes. The increase in length at which the transition occurred was similar in EDL and SOL, however, the tension at the transition was greater in SOL than EDL.

in the initial slope between EDL (20.7 ± 1.1 P_o/L_o) and SOL (27.5 ± 3.0 P_o/L_o; $P < 0.05$). This is consistent with a significantly greater crossbridge contribution to FE as revealed by analysis of P_L. The slope of the tension rise after the transition was not significantly different between EDL (3.3 ± 0.5 P_o/L_o) and SOL (4.5 ± 0.5 P_o/L_o; $P > 0.05$). These data are comparable to that reported for small bundles of rat fast skeletal muscle (≈40 P_o/L_o for the initial slope and ≈5 P_o/L_o for the latter rise[2]). The slightly lower values in our study likely reflect an increased compliance due to the larger muscle preparations and tendon contributions used here.

In some traces (particularly those at stretch velocities of ≈1–5 $L_o s^{-1}$) it was possible to clearly identify the transition between the steep and slow force increases on the rising phase. At velocities below 1 $L_o s^{-1}$ the transition was very gradual and resulted in a curvature in the force response instead of a sharp transition point. At velocities greater than 5 $L_o s^{-1}$, the transition point approached the end of the ramp stretch, and the latter phase was difficult to distinguish clearly. At the intermediate velocities the transition point was characterized by identifying the intersection of two linear regression lines fit to the initial and latter slopes. The length at which this transition occurred was similar for SOL (0.025 ± 0.001 L_o) and EDL (0.027 ± 0.001 L_o). The force at this transition was significantly greater for SOL (0.53 ± 0.03 P_o) than EDL (0.42 ± 0.02 P_o; $P < 0.05$).

Effect of Stretch-Induced Muscle Damage on Force Enhancement. The eccentric contraction protocol significantly reduced P_o in both EDL (by 23.5 ± 4.2%) and SOL (by 11.5 ± 5.2%), however, the decrease was significantly greater for EDL than for SOL ($P < 0.05$; Fig. 6). For EDL, the slope of the initial tension rise was also significantly reduced from 16.1 ± 0.6 P_o/L_o to 13.0 ± 0.6 P_o/L_o after the damage protocol. For SOL there was no significant change in the slope of the initial tension rise after damage (28.0 ± 1.6 P_o/L_o before damage

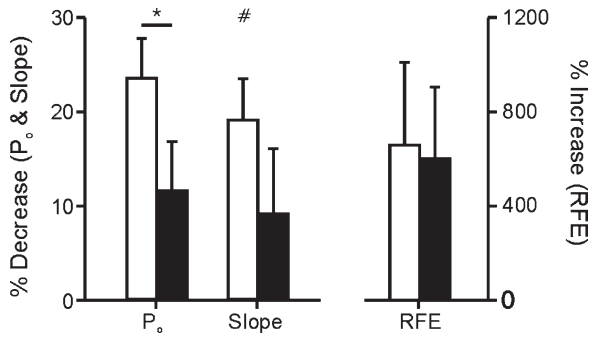

FIGURE 6. The effects of eccentric muscle damage on stretch-induced force enhancement. The mean ±SE decrease in maximum isometric tension (P_o) and slope of the initial tension rise (P_o/L_o) after 10 damaging eccentric contractions are plotted on the left vertical axis for EDL (open bars; $n = 9$) and SOL (filled bars; $n = 9$). The mean ±SE increase in RFE is plotted on the right vertical axis. *Significant difference between EDL and SOL; #Significant decrease in slope after eccentric muscle damage ($P < 0.05$).

compared to 25.9 ± 3.1 P_o/L_o after damage). Despite these differences in force and stiffness changes between EDL and SOL, the amplitude of RFE increased ≈6-fold after damage in both muscles (Fig. 6; $P < 0.01$).

DISCUSSION

FE during stretch has been suggested to arise from strain of contractile and noncontractile components within the sarcomere.[2,6,10] Since fast-twitch and slow-twitch skeletal muscles differ in the properties of both their contractile and noncontractile proteins, we chose to examine the EDL and SOL muscles of adult rats in order to gain a better understanding of the mechanisms of stretch-induced FE and RFE. We have shown that the FE during stretch was significantly greater in the slow SOL than in the fast EDL muscle. This observation can be attributed to a significantly greater contribution of the velocity-dependent contractile component to FE, as revealed from curve-fit analysis (i.e., P_L), as well as the analysis of the slope of the initial tension rise and the tension at the transition between the initial and latter tension rise. RFE after stretch, however, was significantly greater in EDL than SOL and may reflect fiber-type differences in the composition of noncontractile structural proteins that regulate sarcomeric stability.

Contractile Contributions to Force Enhancement. The greater slope of the initial tension rise, or stiffness, that we observed for slow compared to fast muscle has also been reported in single skinned fiber experiments[46] and from in situ experiments on fast and slow motor units in cat muscles.[48] In both cases the increased stiffness in slow muscle was felt to arise from the slower crossbridge cycling rate and, therefore, an increased average strain of all attached crossbridges, based on the Schoenberg[49] model of crossbridge cycling. However, as Malamud et al.[46] point out, for fast skeletal muscle the faster detachment rate of crossbridges during stretch is likely to be offset by a faster reattachment of crossbridges, and therefore the fiber-type differences in stiffness may not be due to crossbridge cycling kinetics alone. Given that the amplitude of FE during stretch is dependent on the calcium concentration[17] and the effects of sarcomere length on calcium sensitivity are different for fast and slow fibers,[50] it is appealing to suggest that this may account for the fiber-type differences in FE shown here. However, our experiments were performed under conditions of maximal activation, where changes in calcium sensitivity are unlikely to have any bearing on force production. Alternatively, Edman[51] has demonstrated that FE during stretch is dependent on the myofilament lattice width, suggesting that the attachment of crossbridges during stretch is enhanced as the lateral spacing between filaments is reduced. Considering that the myosin binding-induced cooperative activation of the thin filament is greater in slow skeletal muscle fibers,[52] such a mechanism may contribute to the observed fiber-type differences in FE.

Linari et al.[53] examined force enhancement characteristics in single skinned fibers from human muscle containing different myosin heavy chain isoforms. In these precisely controlled experiments, the *relative* force enhancement during stretch (i.e., FE normalized to the maximum isometric force) generated by single fibers containing slow MHC-1 was higher than in MHC-2A and 2A/X fibers. However, the increased relative FE could be accounted for by the significantly lower isometric force recorded for MHC-1 fibers, such that the *total* resistance to stretch was similar between fast and slow fibers. In both fiber types the stretch-induced force enhancement was attributed to an increase in the number of attached crossbridges as well as a higher force per crossbridge.[53] In contrast to Linari et al.'s observations, however, the maximum isometric tension in the present study was not significantly different between EDL and SOL. Therefore, the relative force enhancement and the total force enhancement in our study were both greater for SOL than for EDL. The reason for the differences in isometric force and total resistance to stretch between these studies in unclear, although it is worth noting that the experiments of Linari et al.[53] were performed at temperatures much lower than ours (≈12°C vs. ≈25°C), at which the temperature sensitivity of P_o is markedly different for fast and slow fibers.[54]

Regardless of the underlying mechanisms, the strain of attached crossbridges provides a substantial contribution to the resistance of muscle lengthening. The functional benefits of increased stiffness would be significant in slow, type-I fibers, as these are the fibers that will be recruited first and are repeatedly active during postural tasks when the resistance to lengthening is fundamental to the maintenance of posture.

Noncontractile Contribution to Force Enhancement. Numerous models of muscle contraction and crossbridge cycling have been developed that accurately account for the initial tension rise during stretch[2,13,45,47]; however, none of these models predict the continued, slower rise in tension that is often observed when active muscles are stretched beyond ≈1%–2% L_o (e.g., Fig. 5). Therefore, the velocity-independent increase in force during the stretch of active skeletal muscle has been suggested to arise from the strain of noncontractile

component(s) within the sarcomere. Given the documented fiber-type differences in the composition of noncontractile proteins,[41,55] including the expression of the shorter, stiffer titin isoform in fast fibers,[30,31,33,34,56] we hypothesized that the relative contribution of noncontractile proteins to force enhancement would be greater in EDL than soleus muscles. Therefore, it was surprising that there were no fiber-type differences in either the slope of the later force rise or in the component C derived from Eq. (1).

These observations suggest that other noncontractile elements are likely to contribute to the velocity-independent contribution to FE. Indeed, Prado et al.[34] have shown that although the relative contribution of titin to the total passive stiffness is almost twice as large in EDL as it is in SOL, the contribution of extramyofibrillar structures such as collagen was substantially greater in slow muscle. Therefore, the noncontractile contributions to FE during stretch are likely to arise from the combined strain of numerous structural proteins within the sarcomere. Considering the complex interaction between structural proteins such as titin and desmin and z-disc proteins associated with intracellular signaling pathways,[57] further research is warranted to understand the role of noncontractile proteins in the mechanotransduction process.

In contrast to the noncontractile contribution to FE, we observed a fiber-type dependence of RFE after stretch; the amplitude of the RFE was significantly greater in EDL than SOL. It has been argued that the strain of a noncontractile elastic element develops during the stretch and makes a contribution to FE that is dependent on stretch amplitude.[2,6] At the end of the stretch this force decays, but only partially, such that the steady-state RFE after stretch is a remnant of the elastic force that develops during stretch. Therefore, the origin of RFE may depend on the stress relaxation characteristics of the noncontractile components that contribute to the stretch-induced FE.

To examine this concept further, we determined the relationship between the noncontractile contribution to FE during stretch (i.e., component C from Eq. 1) and the noncontractile contribution to tension that remains after the stretch, i.e., RFE. When RFE is expressed as a ratio of C, the proportion of the noncontractile tension developed during stretch that remains after the stretch was 0.26 for EDL and 0.14 for SOL. Thus, the noncontractile component decays more for SOL than for EDL. Due to its known calcium sensitivity, the stiffness of titin will remain elevated as long as the muscle activation is maintained. Therefore, the differential expression of titin isoforms may contribute to the fiber type differences in RFE to a greater extent than other noncontractile proteins.

An alternative explanation for the origin of RFE is the development of sarcomere length heterogeneity during stretch. This would be consistent with the sarcomere popping theory proposed by Morgan.[8,58] This theory is based on the inherent instability that has been observed in skeletal muscle when it is stretched to long lengths, where further lengthening results in a decrease in overlap between thick and thin filaments and an increase in the strain of passive structural elements such as titin.[8,58] Therefore, the inherent instability of the sarcomere may influence the development of sarcomere length heterogeneity and RFE.

Fiber-type differences in the width and composition of the z-discs[59] and m-bands,[60] along with a higher relative content of intermediate filament proteins such as desmin[41] and dystrophin and associated proteins[55] have been suggested to enhance sarcomere stability in slow muscle.[60] That being the case, we hypothesized that a series of damaging eccentric contractions would compromise the sarcomere stability and resistance to lengthening, thus leading to nonuniform sarcomere lengthening and increased strain of noncontractile proteins in the fast skeletal muscle. This was supported by our observations of the change in contractile and noncontractile contributions to stretch-induced force enhancement following the eccentric damage protocol (see Fig. 6). The decrease in P_o and in the slope of the initial tension rise reflects a reduction in the integrity of the contractile apparatus and coincides with a 6-fold increase in the amplitude of RFE. The impairment of contractile function was significantly greater for EDL than for SOL, which is consistent with an increased susceptibility of fast skeletal muscle to stretch-induced muscle damage. However, despite the increased muscle damage in EDL, it was surprising to note that the relative increase in RFE was similar for both fast and slow muscles. Clearly, further research is warranted to delineate the contribution of various noncontractile proteins to stretch-induced force enhancement. However, we propose that an increased strain of noncontractile proteins is likely to contribute to the 6-fold increase in RFE following damaging eccentric contractions.

In conclusion, the greater contribution of contractile proteins to the force enhancement during stretch in the slow soleus muscle reflects an increase in stiffness or enhanced resistance to muscle lengthening that would be beneficial for the maintenance of posture. RFE, however, was significantly greater in the fast EDL muscle and increased ≈6-fold after a series of damaging eccentric contractions. The strain of noncontractile

proteins provides a means of transmitting mechanical loading to the z-disc, thereby influencing signaling molecules associated with cellular hypertrophy. Therefore, RFE may represent a physiological characteristic of skeletal muscle that facilitates the activation of signaling pathways involved in muscle adaptation and remodeling during eccentric exercise. An understanding of the mechanisms of muscle damage and of pathway(s) by which eccentric exercise leads to muscle adaptation may provide new strategies to aid the development of therapeutic interventions to ameliorate the extent of muscle damage in clinical conditions.

REFERENCES

1. Edman KAP, Elzinga G, Noble MIM. Enhancement of mechanical performance by stretch during tetanic contractions of vertebrate skeletal muscle fibres. J Physiol 1978;281:139–155.
2. Pinniger G, Ranatunga K, Offer G. Crossbridge and non-crossbridge contributions to tension in lengthening rat muscle: force-induced reversal of the power stroke. J Physiol 2006;573(Pt 3):627–643.
3. Roots H, Offer G, Ranatunga K. Comparison of the tension response to ramp shortening and lengthening in intact mammalian muscle fibres: crossbridge and non-crossbridge contributions. J Muscle Res Cell Motil 2008;28:123–139.
4. Abbott B, Aubert X. The force exerted by active striated muscle during and after change of length. J Physiol 1952;117:77–86.
5. Edman KAP, Elzinga G, Noble MI. Residual force enhancement after stretch of contracting frog single muscle fibers. J Gen Physiol 1982; 80:769–784.
6. Edman KAP, Tsuchiya T. Strain of passive elements during force enhancement by stretch in frog muscle fibres. J Physiol 1996;490: 191–205.
7. Herzog W, Lee E, Rassier D. Residual force enhancement in skeletal muscle. J Physiol 2006;574:635–642.
8. Morgan DL. An explanation for residual increased tension in striated-muscle after stretch during contraction. Exp Physiol 1994;79: 831–838.
9. Bagni MA, Cecchi G, Colombini B. Crossbridge properties investigated by fast ramp stretching of activated frog muscle fibres. J Physiol 2005;565:261–268.
10. Flitney F, Hirst D. Crossbridge detachment and sarcomere 'give' during stretch of active frog's muscle. J Physiol 1978;276:449–465.
11. Katz B. The relation between force and speed in muscular contraction. J Physiol 1939;96:45–64.
12. Lombardi V, Piazzesi G. The contractile response during steady lengthening of stimulated frog muscle fibres. J Physiol 1990;431: 141–171.
13. Piazzesi G, Francini F, Linari M, Lombardi V. Tension transients during steady lengthening of tetanised muscle fibres of the frog. J Physiol 1992;445:659–711.
14. Sugi H. Tension changes during and after stretch in frog muscle fibres. J Physiol 1972;225:237–253.
15. Joyce GC, Rack PMH, Westbury DR. The mechanical properties of cat soleus muscle during controlled lengthening and shortening movements. J Physiol 1969;204:461–474.
16. Rack P, Westbury D. The short range of stiffness of active mammalian muscle and its effect on mechanical properties. J Physiol 1974; 240:331–350.
17. Stienen GJ, Versteeg PG, Papp Z, Elzinga G. Mechanical properties of skinned rabbit psoas and soleus muscle fibres during lengthening: effects of phosphate and Ca^{2+}. J Physiol 1992;451:503–523.
18. Rassier DE, Herzog W, Pollack GH. Stretch-induced force enhancement and stability of skeletal muscle myofibrils. Adv Exp Med Biol 2003;538:501–515.
19. Pinniger G, Cresswell A. Residual force enhancement after lengthening is present during submaximal plantar flexion and dorsiflexion actions in humans. J Appl Physiol 2007;102:18–25.
20. Huxley A. Muscle structure and theories of contraction. Prog Biophys Biophys Chem 1957;7:255–318.
21. Linari M, Lucii L, Reconditi M, Vannicelli Casoni ME, Amenitsch H, Bernstorff S, et al. A combined mechanical and X-ray diffraction study of stretch potentiation in single frog muscle fibres. J Physiol (Lond) 2000;526:589–596.
22. Lee E, Herzog W. Residual force enhancement exceeds the isometric force at optimal length for optimized stretch conditions. J Appl Physiol 2008;105:457–462.
23. Mehta A, Herzog W. Cross-bridge induced force enhancement? J Biomech 2008;41:1611–1615.
24. Pinniger G, Bruton JD, Westerblad H, Ranatunga K. Effects of a myosin-II inhibitor (N-benzyl-p-toluene sulfonamide, BTS) on contractile characteristics of intact fast-twitch muscle fibres. J Muscle Res Cell Motil 2005;26:135–141.
25. Sugi H, Tsuchiya T. Stiffness changes during enhancement and deficit of isometric force by slow length changes in frog skeletal muscle fibres. J Physiol 1988;407:215–229.
26. Lehti T, Kalliokoski R, Komulainen J. Repeated bout effect on the cytoskeletal proteins titin, desmin, and dystrophin in rat skeletal muscle. J Muscle Res Cell Motil 2007;28:39–47.
27. Bagni MA, Cecchi G, Colombini B, Colomo F. A non-cross-bridge stiffness in activated frog muscle fibers. Biophys J 2002;82:3118–3127.
28. Herzog W, Leonard TR. Force enhancement following stretching of skeletal muscle: a new mechanism. J Exp Biol 2002;205:1275–1283.
29. Herzog W, Schachar R, Leonard TR. Characterization of the passive component of force enhancement following active stretching of skeletal muscle. J Exp Biol 2003;206:3635–3643.
30. Horowits R, Kempner E, Bisher M, Podolsky R. A physiological role for titin and nebulin in skeletal muscle. Nature 1986;323:160–164.
31. Horowits R. Passive force generation and titin isoforms in mammalian skeletal muscle. Biophys J 1992;61:392–398.
32. Maruyama K, Matsubara S, Natori R, Nonomura Y, Kimura S, Ohashi K, et al. Connectin, an elastic protein of muscle: characterization and function. J Biochem 1977;82:317–337.
33. Mutungi G, Ranatunga K. The viscous, viscoelastic and elastic characteristics of resting fast and slow mammalian (rat) muscle fibres. J Physiol 1996;496:827–836.
34. Prado L, Makarenko I, Andresen C, Kruger M, Opitz CA, Linke WA. Isoform diversity of giant proteins in relation to passive and active contractile properties of rabbit skeletal muscle. J Gen Phys 2005;126:461–480.
35. Macpherson PC, Schork MA, Faulkner JA. Contraction-induced injury to single fiber segments from fast and slow muscles of rats by single stretches. Am J Physiol Cell Physiol 1996;271:C1438–1446.
36. Eng CM, Smallwood LH, Rainiero MP, Lahey M, Ward SR, Lieber RL. Scaling of muscle architecture and fiber types in the rat hindlimb. J Exp Biol 2008;211:2336–2345.
37. Close R. Dynamic properties of fast and slow skeletal muscle of rat during development. J Physiol 1964;173:74–95.
38. Ranatunga K, Thomas P. Correlation between shortening velocity, force-velocity relation and histochemical fibre-type composition in rat muscles. J Muscle Res Cell Motil 1990;11:240–250.
39. Wigston D, English A. Fibre-type proportions in mammalian soleus muscle during postnatal development. J Neurobiol 1991;23:61–70.
40. Schiaffino S, Reggiani C. Myosin isoforms in mammalian skeletal muscle. J Appl Physiol 1994;77:493–501.
41. Chopard A, Pons F, Marini J-F. Cytoskeletal protein contents before and after hindlimb suspension in a fast and slow rat skeletal muscle. Am J Physiol Regul Integr Comp Physiol 2001;280:R323–330.
42. Peters D, Barash IA, Burdi M, Yuan PS, Mathew L, Friden J, et al. Asynchronous functional, cellular and transcriptional changes after a bout of eccentric exercise in the rat. J Physiol 2003;553:947–957.
43. Segal SS, White TP, Faulkner JA. Architecture, composition, and contractile properties of rat soleus muscle grafts. Am J Physiol Cell Physiol 1986;250:C474–479.
44. Schoenberg M. Equilibrium muscle cross-bridge behaviour. Biophys J 1985;48:467–475.
45. Getz EB, Cooke R, Lehman SL. Phase transition in force during ramp stretches of skeletal muscle. Biophys J 1998;75:2971–2983.
46. Malamud JG, Godt RE, Nichols TR. Relationship between short-range stiffness and yielding in type-identified, chemically skinned muscle fibers from the cat triceps surae muscles. J Neurophysiol 1996;76:2280–2289.
47. Månsson A. The tension response to stretch of intact skeletal muscle fibres of the frog at varied tonicity of the extracellular medium. J Muscle Res Cell Motil 1994;15:145–157.
48. Petit J, Filippi GM, Emonet-Denand F, Hunt CC, Laporte Y. Changes in muscle stiffness produced by motor units of different types in peroneus longus muscle of cat. J Neurophysiol 1990;63:190–197.
49. Schoenberg M. Characterization of the myosin adenosine triphosphate (M.ATP) crossbridge in rabbit and frog skeletal muscle fibers. Biophys J 1988;54:135–148.
50. Stephenson DG, Williams DA. Effects of sarcomere length on the force—pCa relation in fast- and slow-twitch skinned muscle fibres from the rat. J Physiol 1982;333:637–653.
51. Edman KAP. The force bearing capacity of frog muscle fibres during stretch: its relation to sarcomere length and fibre width. J Physiol 1999;519:515–526.
52. Metzger JM. Myosin binding-induced cooperative activation of the thin filament in cardiac myocytes and skeletal muscle fibers. Biophys J 1995;68:1430–1442.
53. Linari M, Bottinelli R, Pellegrino M, Reconditi M, Reggiani C, Lombardi V. The mechanism of the force response to stretch in human skinned fibres with different myosin isoforms. J Physiol 2003;554:335–352.

54. Ranatunga KW. Influence of temperature on isometric tension development in mouse fast- and slow-twitch skeletal muscles. Exp Neurol 1980;70:211–218.
55. Ho-Kim M-A, Rogers PA. Quantitative analysis of dystrophin in fast- and slow-twitch mammalian skeletal muscle. FEBS Lett 1992;304: 187–191.
56. Freiburg A, Trombitas K, Hell W, Cazorla O, Fougerousse F, Centner T, et al. Series of exon-skipping events in the elastic spring region of titin as the structural basis for myofibrillar elastic diversity. Circ Res 2000;86:1114–1121.
57. Frank D, Kuhn C, Katus H, Frey N. The sarcomeric Z-disc: a nodal point in signalling and disease. J Mol Med 2006;84:446–468.
58. Morgan DL. New insights into the behavior of muscle during active lengthening. Biophys J 1990;57:209–221.
59. Luther PK, Padrón R, Ritter S, Craig R, Squire JM. Heterogeneity of z-band structure within a single muscle sarcomere: implications for sarcomere assembly. J Mol Biol 2003;332:161–169.
60. Agarkova I, Ehler E, Lange S, Schoenauer R, Perriard J-C. M-band: a safeguard for sarcomere stability? J Muscle Res Cell Motil 2003;24: 191–203.